Bioorganic & Medicinal Chemistry Letters 24 (2014) 4001–4005

Contents lists available at ScienceDirect

Bioorganic & Medicinal Chemistry Letters

journal homepage: www.elsevier.com/locate/bmcl

Molecular dynamics study-guided identification of cyclic amine structures as novel hydrophobic tail components of hPPARγ agonists

Yuta Tanaka [a,†], Kanae Gamo [a,†], Takuji Oyama [b], Masao Ohashi [a], Minoru Waki [a], Kenji Matsuno [a], Nobuyasu Matsuura [c], Hiroaki Tokiwa [d], Hiroyuki Miyachi [a,*]

[a] Graduate School of Medicine, Dentistry and Pharmaceutical Sciences, Okayama University, 1-1-1, Tsushima-Naka, Kita-ku, Okayama 700-8530, Japan
[b] Department of Biotechnology, Faculty of Life and Environmental Sciences, University of Yamanashi, 4-3-37 Takeda, Kofu City, Yamanashi 400-8510, Japan
[c] Department of Life Science, Faculty of Science, Okayama University of Science, 1-1 Ridai-cho, Kita-ku, Okayama 700-0005, Japan
[d] Department of Chemistry, Rikkyo University, Nishi-Ikebukuro, Toshimaku, Tokyo 171-8501, Japan

ARTICLE INFO

Article history:
Received 17 May 2014
Revised 5 June 2014
Accepted 9 June 2014
Available online 24 June 2014

Keywords:
Peroxisome proliferator-activated receptor gamma
Cyclic amine
Molecular dynamics simulation

ABSTRACT

We previously reported that a α-benzylphenylpropanoic acid-type hPPARγ-selective agonist with a piperidine ring as the hydrophobic tail part (**3**) exhibited sub-micromolar-order hPPARγ agonistic activity. In order to enhance the activity, we planned to carry out structural development based on information obtained from the X-ray crystal structure of hPPARγ ligand binding domain (LBD) complexed with **3**. However, the shape and/or nature of the binding pocket surrounding the piperidine ring of **3** could not be precisely delineated because the structure of the omega loop of the LBD was poorly defined. Therefore, we constructed and inserted a plausible omega loop by means of molecular dynamics simulation. We then used the reconstructed LBD structure to design new mono-, bi- and tricyclic amine-bearing compounds that might be expected to show greater binding affinity for the LBD. Here, we describe synthesis and evaluation of α-benzylphenylpropanoic acid derivatives **8**. As expected, most of the newly synthesized compounds exhibited more potent hPPARγ agonistic activity and greater hPPARγ binding affinity than **3**. Some of these compounds also showed comparable aqueous solubility to **3**.

Structural biology data obtained by X-ray crystallographic analysis of target protein(s) complexed with specific ligand(s) are a powerful tool for medicinal chemists, offering insight into the shape of the ligand-binding pocket, critical amino acids for ligand binding, specific interaction modes of ligands, determinants of potency and/or selectivity, and so on. Such information provides a basis for medicinal chemists to design structural frameworks for the creation of new lead compounds, and to identify appropriate functional groups for obtaining high potency and/or selectivity. In some cases however, probably due to molecular flexibility or thermodynamic instability, sufficient information about parts of the structure may be unavailable from crystallographic study (Fig. 2A–C).[1–3] This proved to be the case for the omega loop part in the crystal structure of the ligand binding domain (LBD) of human peroxisome proliferator-activated receptor gamma (hPPARγ) complexed with the selective agonist **3**. Here, we describe construction of a plausible structure of the disordered peptide fragment, that is, the omega loop part of hPPARγ, by means of molecular dynamics (MD) calculations. We also describe the discovery of novel active hydrophobic tail structures for our phenylpropanoic acid-type hPPARγ agonists based on the MD-developed hPPARγ model structure.

We have been engaged in structural development studies of various synthetic hPPARs ligands,[4–7] and one of our current focuses is creation of hPPARγ agonists and hPPARγ antagonists with potent and selective hPPARγ affinity and sufficient aqueous solubility for in vivo use. We recently showed that a α-benzylphenylpropanoic acid-type hPPARγ-selective agonist with a piperidine ring as a hydrophobic tail part (**3**) exhibited sub-micromolar-order hPPARγ agonistic activity with moderate aqueous solubility (Fig. 1).

In order to improve the activity, we planned to modify **3** based on the X-ray crystal structure of hPPARγ LBD complexed with **3** (PDB: 3VSP). However, we found that the structure of some of the amino acids involved in part of the binding pocket surrounding the piperidine ring of **3** was insufficiently well defined (Fig. 2D), because the structure of the omega loop part[8] (265Lys-His-Ile-Thr-Pro-Leu-Gln-Glu-Gln-Ser-275Lys) of the binding pocket was unclear. This is not a special case, because all the hPPAR subtype LBD-ligand complexes examined by our group lack a well-defined omega loop structure, presumably due to molecular flexibility or

* Corresponding author. Tel.: +81 086 251 7930.
E-mail address: miyachi@pharm.okayama-u.ac.jp (H. Miyachi).
† These authors contributed equally.

http://dx.doi.org/10.1016/j.bmcl.2014.06.023
0960-894X/

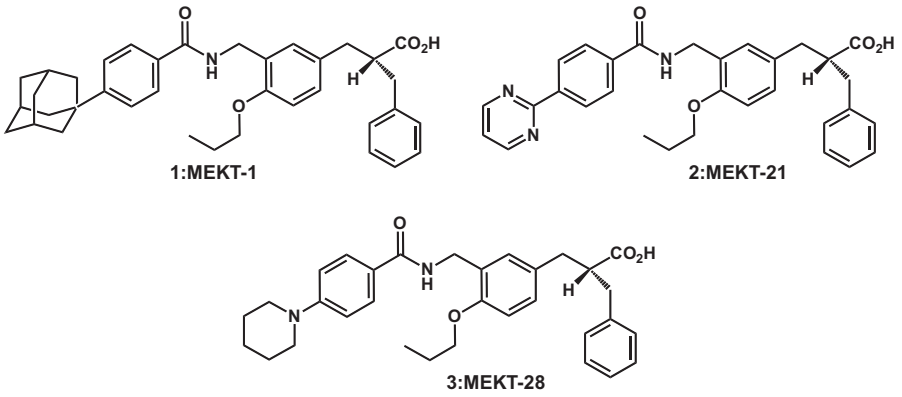

Figure 1. Some representative structures of our previously developed PPARγ agonists. Compound **1**: MEKT-1. Compound **2**: MEKT-21. Compound **3**: MEKT-28.

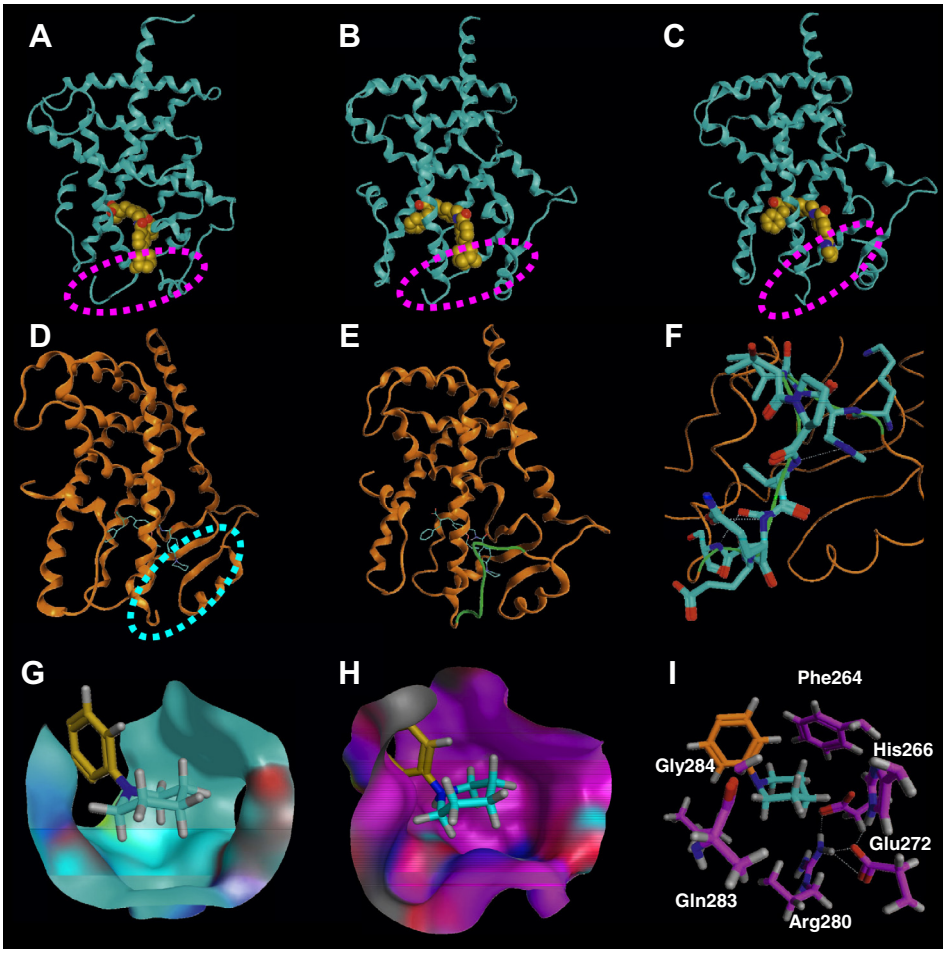

Figure 2. (A)–(D) Crystal structures of hPPARγ LBD–TIPP-703 complex (A) (PDB: 2ZNO), hPPARγ LBD–**1** complex (B) (PDB: 3AN4), hPPARγ LBD–**2** complex (C) (PDB: 3VSO) and hPPARγ LBD–**3** complex (D) (PDB: 3VSP). (E) Whole structure of the omega-loop-inserted hPPARγ LBD–**3** complex model. The main chain of the inserted omega loop structure is depicted as a green ribbon-model. (F) Zoomed view of the reconstructed omega loop structure of hPPARγ LBD. The amino acids of the reconstructed omega loop are depicted as blue cylinder models. (G) The surface structure of the binding pocket surrounding the piperidine ring of **3** in the hPPARγ LBD–**3** complex. (H) The surface structure of the binding pocket surrounding the piperidine ring of **3** in the reconstructed, omega-loop-inserted hPPARγ LBD–**3** complex model. (I) Zoomed view of the piperidine-interacting amino acids in the omega loop-inserted hPPARγ LBD–**3** complex model.

thermodynamic instability, as illustrated in Figure 2A–C. Therefore, we decided to construct and insert a plausible omega loop part by using molecular dynamics (MD) simulation. MD-assisted construction of the omega loop part involved three steps, as follows. (1) We used the molecular operating system (MOE) program suite to insert the eleven amino acids of the omega loop, Lys-His-Ile-Thr-Pro-Leu-Gln-Glu-Gln-Ser-Lys, between the end of the H2′ helix and the beginning of the H3 helix in the PDB: 3VSP protein structure based on the homology alignment method with the use of the template structure (PDB ID: 3VSP) to construct the initial geometry of the omega loop of hPPARγ. (2) Next, compound **3** was docked into this initial geometry of hPPARγ by the ASEDock[9] procedure

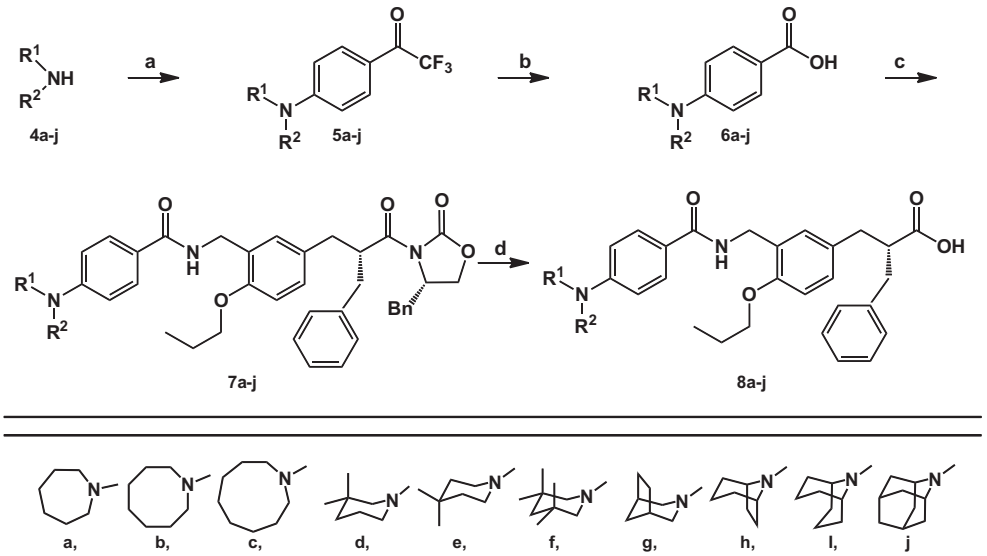

Scheme 1. Synthetic route to the present series of compounds. Reagents and conditions: (a) 2,2,2,4′-tetrafluoroacetophenone, TEA, DMSO, 100 °C, 16 h; (b) NaOH, DMF/H_2O, 100 °C, 2 h, 43–79% (2 steps); (c) (*S*)-3-((*R*)-2-(3-(aminomethyl)-4-propoxybenzyl)-3-phenylpropanoyl)-4-benzyloxazolidin-2-one hydrochloride, HATU, DIEA, DMF, 16 h, 55–95%; (d) LiOH-H_2O, 30% H_2O_2, THF/H_2O, 3.5 h, 46–94%.

Table 1
Values of hPPARs transactivation activity (EC_{50}), binding affinity (K_D) and aqueous solubility of the present series of derivatives

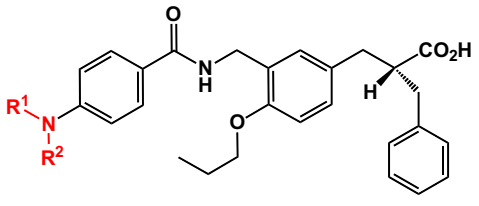

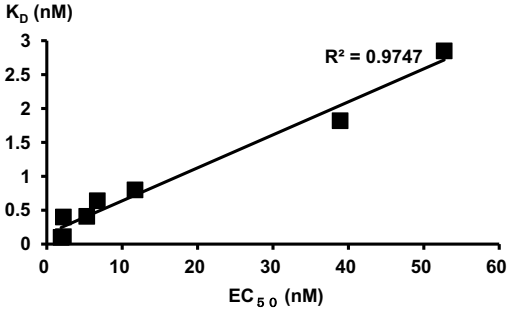

Compd	R^1R^2N-	EC_{50}[a] (nM)	K_D[b] (nM)	Sol.pH7.4[c] (μg/mL)	Compd	R^1R^2N-	EC_{50}[a] (nM)	K_D[b] (nM)	Sol.pH7.4[c] (μg/mL)
3		52.7	2.85	10	**8f**	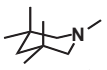	2.2	0.40	<10
8a		6.7	n.t	n.t	**8g**		6.7	0.64	10
8b	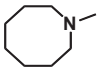	1.9	0.1	<10	**8h**		5.3	0.41	<10
8c	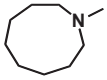	38.9	1.82	n.t	**8i**		11.7	0.80	10
8d	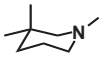	7.0	n.t	<10	**8j**		2.2	0.11	<10
8e	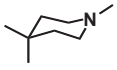	10.4	n.t	<10	**1**	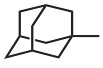	3.6	N.T.	<1

[a] EC_{50} values represent half-maximal effective concentration (nM). These data were taken from the two independent duplicated experiments.
[b] K_D values were measured using the surface plasmon resonance (SPR) method (Biacore X100). These data were taken from the two independent duplicated experiments.
[c] Solubility was measured using the 48 h shaking flask method. 1 mg of compound was ground in an agate mortar and taken up in 1.0 mL of an equal volume of a mixture of phosphate buffer (pH 7.2–7.4) and EtOH. The suspension was shaken for 48 h at 25 °C. An aliquot was filtered through a Minisart RC 15 (0.45 μm). The filtrate was diluted in CH_3CN and subjected to HPLC with UV detection at 254 nm. The concentration of the sample solution was calculated using a previously determined calibration curve, corrected for the dilution factor of the sample.

incorporated in the MOE program suite to obtain the structure of the hPPARγ complex with compound **3**, and the complex structure having the top docking score was adopted. (3) Thermal relaxation of the complex was performed by means of isothermal (NVT) MD simulations under standard conditions. The temperature and pressure of the system were controlled by Nos'e-Poincar'e-Andersen

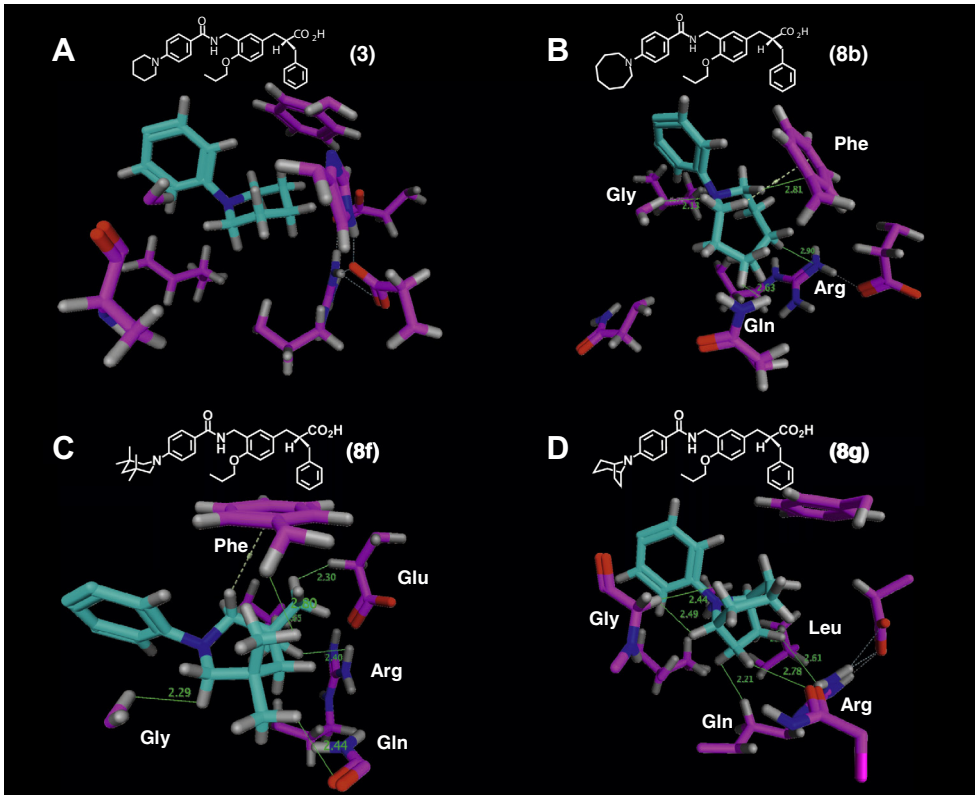

Figure 3. (A)–(D) Zoomed view of the molecular modeling structures of **3**, **8b**, **8f** and **8g** complexed with the omega-loop-inserted hPPARγ LBD. The amino acids of the binding cavity are depicted as magenta cylinder models, and the structures of the ligands are depicted as cyan cylinder models.

formalism (details will be reported elsewhere). The structure of the omega loop-reconstructed hPPARγ LBD complexed with **3** is depicted in Figure 2E, and a magnified view of the reconstructed omega loop structure is shown in Figure 2F. The surface structures of the binding pocket surrounding the piperidine ring of **3** in the hPPARγ LBD–**3** complex and in the omega loop-reconstructed hPPARγ LBD–**3** complex model are depicted in Figure 2G and H, respectively.

The binding pocket surrounding the piperidine ring is somewhat narrower in the MD-assisted binding model, as compared with the model obtained from the X-ray crystal structure. However, there is still remaining hydrophobic space, especially around the 2,3,5,6 positions of the piperidine ring of **3**. Therefore, we speculated that compounds bearing ring-expanded, bicyclic, and tricyclic amine derivatives, **8a–j**, might exhibit superior hPPARγ agonistic activity.

To test this idea, we synthesized the series of compounds illustrated in Scheme 1. The appropriate amine[10] was treated with 2,2,2,4′-tetrafluoroacetophenone in the presence of triethylamine in DMSO to afford the amino group-substituted 2,2,2-trifluoroacetophenone, and then alkaline hydrolysis[11] afforded the key intermediate benzoic acids **6a–j**. Compounds **6a–j** were condensed with (*S*)-3-((*R*)-2-(3-(aminomethyl)-4-propoxybenzyl)-3-phenylpropanoyl)-4-benzyloxazolidin-2-one hydrochloride,[3] followed by LiOOH hydrolysis[12] to afford the desired compounds **8a–j**.

First of all, we focused on the ring size-expanded series, **8a–8c**. As shown in Table 1, the ring size of the cyclic amino group correlated with hPPARγ agonistic activity, which increased in the ring-size order of 6 (**3**) < 7 (**8a**) < 8 (**8b**). The 8-membered cyclic amino group (**8b**) might be optimal, because the 9-membered cyclic amino group (**8c**) exhibited decreased hPPARγ agonistic activity, although it still possessed potent hPPARγ agonistic activity, comparable to that of **3**.

As expected, the introduction of a dimethyl group at the 3- and 4-positions of the piperidine ring of **3** was also effective in increasing hPPARγ agonistic activity. The 3,3-dimethylpiperidine- and 4,4-dimethylpiperidine derivatives (**8d**, **8e**) exhibited superior activity, and the potency of 3,3,5,5-tetramethylpiperidine derivative (**8f**) was more than 10 times greater than that of **3**.

Based on these results, we next synthesized bicyclic and tricyclic amine structures (**8g–8j**). All these compounds exhibited greater hPPARγ agonistic activity than **3**. Representative compounds, **8b**, **8f** and **8j**, exhibited potent hPPARγ agonistic activity, comparable to that of a previously reported α-benzylphenylpropanoic acid-type hPPARγ-selective agonist with a bulky adamantyl group as the hydrophobic tail part (**1**).[1]

To understand the structure–activity relationship of the present series of compounds, we constructed binding models of representative compounds (**8b**, **8f** and **8g**) complexed with the omega loop-reconstructed hPPARγ LBD, using the computational ligand-docking program ASEdock incorporated in the MOE program suite. We calculated the interaction energy of each conformer with the omega loop-reconstructed hPPARγ LBD, and the top energy-minimized conformer was selected in each case. The results are summarized in Figure 3A–D, in addition to that for the omega loop-reconstructed hPPARγ LBD–**3** complex model.

As described above, the piperidine ring of **3** is hosted in the hydrophobic binding cavity composed of the side chains of amino acid residues Glu259, Phe264, His266, Glu272, Arg280, Ile281, Gln283 and Gly284 (Fig. 3A). Expansion of the ring size of the hydrophobic tail part amino moiety from 6 (**3**) to 8 (**3b**) enhanced the hydrophobic interaction, especially with the side chains of Phe264, Arg280, Gln283 and Gly284 (Fig. 3B). On the other hand, in the case of **3c**, both methylenes adjacent to the nitrogen atom of the cyclononyl amino moiety showed short contacts with the side chains of Phe264 and Gly284. The introduction of tetramethyl

groups at the 3,3,5,5 positions of the piperidine ring of **3** enhanced the hydrophobic interactions with Phe264, Glu272, Arg280, Gln283 and Gly284 (Fig. 3C). The formation of a bicyclic ring system also enhanced the hydrophobic interactions with the side chains of Arg280, Gln283 and Gly284 (Fig. 3D). All these data indicated that the introduction of appropriate hydrophobic substituents at suitable positions on the piperidine ring of **3** effectively enhances the hydrophobic interactions with the binding cavity of the omega loop-reconstructed hPPARγ LBD.

In order to confirm that the increase in hPPARγ agonistic activity is due to increased binding affinity for hPPARγ owing to introduction of the additional alkyl groups, we then evaluated the direct binding affinity (K_D) of representative compounds to hPPARγ[13] (we used the nitrilotriacetic acid (NTA) sensor chip method to avoid non-specific binding of the ligand to hPPARγ LBD). As shown in Table 1, compound **3** exhibited nanomolar-order K_D value, and representative compounds of the present series, **8b**, **8f**, **8g**, **8h**, **8i** and **8j**, all exhibited sub-nanomolar-order K_D values, except **8c**. The in vitro hPPARγ agonistic activity (EC_{50}) was well correlated with the binding affinity (K_D) ($r^2 = 0.97$), suggesting that the increase in hPPARγ agonistic activity of the present series of compounds is indeed mainly due to increased binding affinity for hPPARγ Table 1.

We then evaluated the thermodynamic solubility of representative compounds.[14] Although most of the potent compounds exhibited decreased aqueous solubility, 8-azabicyclo[3,2,1]octane derivative (**8g**) showed aqueous solubility comparable to that of the parent piperidine derivative (**3**).

In conclusion, we have succeeded in constructing a plausible omega loop structure for the hPPARγ LBD by means of MD simulation. We used the reconstructed hPPARγ LBD model structure to design new mono-, bi- and tri-cyclic amine compounds that were expected to show increased binding affinity for the LBD. As expected, most of the newly designed and synthesized compounds exhibited more potent hPPARγ agonistic activity and greater hPPARγ binding affinity than **3**. Some of these compounds exhibited comparable aqueous solubility to **3**. In order to ascertain the precise binding mode of the representative compound **8g**, we are currently attempting an X-ray crystallographic analysis of the hPPARγ LBD complexed with **8g**.

Acknowledgments

This work was supported in part by a Grant-in-Aid for Scientific Research from The Ministry of Education, Culture, Sports, Science and Technology, Japan, and Platform for Drug Discovery, Informatics, and Structural Life Science from the Ministry of Education, Culture, Sports, Science and Technology, Japan.

References and notes

1. Kasuga, J.; Yamasaki, D.; Ogura, K.; Shimizu, M.; Sato, M.; Makishima, M.; Doi, T.; Hashimoto, Y.; Miyachi, H. *Bioorg. Med. Chem. Lett.* **2008**, *18*, 1110.
2. Ohashi, M.; Oyama, T.; Nakagome, I.; Sato, M.; Nishio, Y.; Nobusada, H.; Hirono, S.; Morikawa, K.; Hashimoto, Y.; Miyachi, H. *J. Med. Chem.* **2011**, *54*, 331.
3. Ohashi, M.; Oyama, T.; Putranto, E. W.; Waku, T.; Nobusada, H.; Kataoka, K.; Matsuno, K.; Yashiro, M.; Morikawa, K.; Huh, N. H.; Miyachi, H. *Bioorg. Med. Chem.* **2013**, *21*, 2319.
4. Ban, S.; Kasuga, J.; Nakagome, I.; Nobusada, H.; Takayama, F.; Hirono, S.; Kawasaki, H.; Hashimoto, Y.; Miyachi, H. *Bioorg. Med. Chem.* **2011**, *19*, 3183.
5. Kasuga, J.; Yamasaki, D.; Araya, Y.; Nakagawa, A.; Makishima, M.; Doi, T.; Hashimoto, Y.; Miyachi, H. *Bioorg. Med. Chem.* **2006**, *14*, 8405.
6. Kasuga, J.; Nakagome, I.; Aoyama, A.; Sako, K.; Ishizawa, M.; Ogura, M.; Makishima, M.; Hirono, S.; Hashimoto, Y.; Miyachi, H. *Bioorg. Med. Chem.* **2007**, *15*, 5177.
7. Kasuga, J.; Oyama, T.; Nakagome, I.; Makishima, M.; Hirono, S.; Morikawa, K.; Hashimoto, Y.; Miyachi, H. *ChemMedChem* **2008**, *3*, 1662.
8. Waku, T.; Shiraki, T.; Oyama, T.; Maebara, K.; Nakamori, R.; Morikawa, K. *EMBO J.* **2010**, *29*, 3395.
9. Goto, J.; Kataoka, R.; Muta, H.; Hirayama, N. *J. Chem. Inf. Model.* **2008**, *48*, 583.
10. (a) (a) 3,3,5,5-Tetramethylpiperidine: Mizuno, M.; Manabe, A., WO 2004099160 (A1).; (b) (b) 8-Azabicyclo[3,2,1]octane hydrochloride: Mueller, R.; Street, L., WO 2009/023126 (A2).; 8-Azabicyclo[3,3,1]nonane hydrochloride: (c) Markus, B. L.; Shannon, S. S. *ACS Catal.* **2013**, *3*, 2612; 3-Azabicyclo[3,2,1]octane hydrochloride: (d) Dong, J.; Han, H.; Geng, B.; Li, X.; Gong, Z.; Liu, K. *J. Pept. Res.* **2005**, *65*, 440; 2-Azaadamantane: (e) Shibuya, M.; Sasano, Y.; Tomizawa, M.; Hamada, T.; Kozawa, M.; Nagahama, N.; Iwabuchi, Y. *Synthesis* **2011**, *21*, 3418. The other cyclic amines were commercial products.
11. Delgado, A.; Clardy, J. *Tetrahedron Lett.* **1992**, *20*, 2789.
12. Evans, D. A.; Bartroli, J.; Shih, T. L. *J. Am. Chem. Soc.* **1981**, *103*, 2127.
13. We performed direct binding assay of representative compounds based on the principle of the surface plasmon resonance, using a Biacore X 100 system with a hPPARγ LBD-functionalized sensor-chip. The experimental protocol was as follows.
Reagents: Reagents ($NiCl_2$, EDTA, NaOH) were purchased from Biacore (Uppsala, Sweden). The assay compounds were prepared as 10 mM stock solutions in DMSO. Immediately before analysis, each compound was diluted with assay buffer containing 10 mM HEPES, 150 mM sodium chloride, 0.05% TWEEN 20, pH 7.4 to yield a final DMSO concentration of 1% and a compound concentration of 1000, 100, 10, 1, 0.1 or 0.01 nM.
Capture of His-hPPARγ LBD by NTA: Biacore X100 flow cells were activated for 1 min by injecting 0.5 mM $NiCl_2$. A 250 μg/mL His-hPPARγ LBD solution (in 10 mM HEPES, 150 mM sodium chloride, pH 7.4) was injected for 2 min at a flow rate of 10 μL/min. Typically, this method resulted in immobilization of ca. 2500 RU PPARγ LBD.
Kinetic analysis of ligand/hPPARγ LBD interactions: To collect detailed kinetic data, a concentration series of each compound was injected at a flow rate of 30 μL/min at 25 °C. For analysis, the association and the dissociation phases were fixed at 60 s.
Analysis: Affinity analysis of each ligand/receptor interaction was conducted by fitting the response data to steady-state affinity according to supplier's protocol.
14. Ishikawa, M.; Hashimoto, Y. *J. Med. Chem.* **2011**, *54*, 1539.